

Application of stereo laser tracking methods for quantifying flight dynamics - II

Timothy J. Miller ^{χ a}, Edward F. Romero ^{α a}, Hubert W. Schreier ^{β b}, and Michael T. Valley ^{δ a}

^a Sandia National Laboratories, PO Box 5800, Albuquerque, NM 87185

^b Correlated Solutions, Inc., 120 Kaminer Way Parkway Suite A, Columbia, SC 29210

ABSTRACT

Conventional tracking systems measure time-space-position data and collect imagery to quantify the flight dynamics of tracked targets. A major obstacle that severely impacts the accuracy of the target characterization is atmospheric turbulence induced distortions of the tracking laser beam and imagery degradations. Tracking occurs in a continuously changing atmosphere resulting in rapid variations in the tracking laser beam and distorted imagery. These atmospheric effects, combined with other degradation affects such as measurement system motion, defocus blur, and spatially varying noise, severely limit the viability and accuracy of many tracking and imagery-based analysis methods. In 2007, using a high speed sled test, we demonstrated the feasibility of quantifying flight dynamics with stereo laser tracking and multi-video imagery in the presence of turbulence and shock waves. The technique acquires stereo views (two or more) of a moving test article that has an applied random speckled (dot) pattern painted on the surface to provide unique tracking points. The stereo views are reconciled via coordinate transformations and correlation of the transformed images. The 2007 results demonstrated that dual laser tracker data can be used to update camera calibration data for stereo imaging to extend the image correlation approach to moving field of view applications such as missile tracking and missile performance characterization such as attitude measurements. However, these results were predominantly qualitative in nature, focusing on the degree of correlation. This paper will present quantitative results from 2008 outdoor centrifuge tests and assess the digital image correlation accuracy for time varying attitude and position measurements.

Keywords: Digital Image Correlation (DIC), Stereo camera system, Atmospheric turbulence, Atmospheric distortion.

1. INTRODUCTION

Sandia National Laboratories laser trackers are being tasked with providing precision attitude and flight dynamics information in addition to their traditional role in supplying time-space-position-information (TSPI) acquired during flight tests¹. This applies to all phases of the trajectory for the given test item, although recent emphasis has been placed on the terminal phase and, in particular, the impact conditions. Ultimately, the trackers are expected to obtain 6-degree-of-freedom measurements together with spin rate, wobble, and other flight related parameters associated with non-rigid body motions. Measurement accuracy requirements vary depending on application, but typical expected positional accuracies are on the scale of inches and angular accuracy requirements are one to two tenths of a degree. These requirements emphasize the need for enhanced capabilities.

Using high-speed digital video cameras and image processing techniques, it may be possible to measure test-unit attitude and surface deformations during key portions of the test-unit's trajectory. Our initial approach is to process position and image data collected from two laser trackers to extract a dense set of three-dimensional points on the surface of the test-unit. Once this is done, the transformations are found that align a set of points from a rigid-body model of the test-unit with the set of corresponding points from the extracted data for each time frame. The transformations required to align the rigid-body model describe the attitude and position of the test-unit in the world coordinate frame.

^χ timille@sandia.gov, Phone 505-284-8194

^α efromer@sandia.gov, Phone: 505-844-7384

^β schreier@correlatedsolutions.com, Phone: 803-926-7272

^δ mtvalle@sandia.gov, Phone: 505-844-1201

In order to evaluate the viability of applying digital image correlation (DIC) techniques on images collected from two laser trackers, we have initiated a phased feasibility study. The first phase, investigated the likelihood of the technique using a rocket sled experiment². The rocket sled experiment confirmed that the technique is possible. The second phase of experiments were designed and conducted to evaluate the accuracy of the technique. This paper focuses on the second phase of testing and some initial results.

In section 2, we review the Dual Laser Tracker DIC (DLTDIC) technique. Section 2 provides background regarding the Sandia National Laboratories laser trackers and Dual Laser Tracker Digital Image Correlation. Section 3 discusses the experimental approach and setup. Sections 4 and 5 present test data and results from the first fully analyzed experiment. Conclusions and next steps are given in section 6.

2. BACKGROUND

2.1 Review of a Sandia National Laboratories laser tracker

Sandia's laser trackers recorded reflected imagery from a 0.4572 m gimballed mirror which servers to direct the tracking laser beam during the test. In addition, the trackers record azimuth, elevation, and range to the test-unit, as well as the horizontal and vertical error signals for every millisecond during the test. The azimuth and elevation values are acquired from 18-bit encoders attached to the gimballed mirror, which resolve to 24 microradians. The range values are quantified in real-time by a ranging system that modulates and processes the tracker's laser beam. The azimuth, elevation, range and error values are post processed using data reduction algorithms^{3,4} to quantify the TSPI of the test-unit and the apparent rotation of the reflect imagery. The apparent camera rotation is a function of the relative positions of the gimballed mirror, the camera, and the tracking position. In other words, the images reflected by the gimballed mirror and captured by the fixed camera rotate and appear as if the camera itself is rotating. Three images from the rocket sled experiment showing the apparent camera rotation are shown in Fig. 1. The apparent camera rotation inherent in the recorder laser tracker imagery is important because it needs to be account for when calculated the three-dimensional position of the dense of points on the test-unit's surface.

For a detailed review of Sandia's laser tracker please see references 1 and 2.



Fig. 1. Images illustrating apparent camera rotation collected from laser tracker at three positions along the sled track

2.2 Dual Laser Tracker Digital Image Correlation

The basic DLTDIC technique involves post processing synchronized image pairs collected from a stereo camera system (i.e., two laser trackers) to calculate the full-field 3D positions on the test-unit's surface, which has a random speckle pattern applied to it. Digital Image Correlation³ (DIC^a) is then applied to find and track corresponding sub-pixel locations of the speckle pattern for each image pair. The sub-pixel correspondences are then triangulated using the intrinsic and extrinsic parameters of the stereo camera system that have been determined for each image pair. The set of triangulate points represent unique positions along the test-unit's surface for each time frame. The transformations are then found that align a rigid-body description of the test-unit with the triangulated points. These transformations formulate the attitude and position of the test-unit for each time frame.

^a DIC is a full-field measurement technique that processes images from a pair of calibrated time-synchronized cameras to estimate the 3D shape, displacement, velocity and strains of a specimen that has been prepared with a high contrast speckle pattern.

The traditional DIC application expects the intrinsic and extrinsic parameters found during a calibration process (for a stationary set of cameras) to remain fixed during the test. This is not the case for images captured from a moving flight test-unit. For this situation, it is necessary to recalculate the relative camera orientation for the image pairs at each time step and assume that the intrinsic parameters remain fixed throughout the test run. Before the test, the intrinsic parameters are quantified using a traditional calibration method.

3. APPROACH

The first phase of the feasibility study focused on the proof of concept of the DLTDIC technique. A rocket sled experiment was conducted to provide laser tracker TSPI data and stereo imagery to test the technique. The initial set of algorithms and processes were developed during the first phase of the study². Later phases will refine the DLTDIC technique and determine the necessary enhancements to the laser trackers to achieve the accuracies required for evaluation of flight system performance.

The second phase of the feasibility study focuses on quantifying the accuracy of the new technique in the presence of atmospheric turbulence. Sled track testing demonstrated that the technique is practical, but the high cost and variability of sled track testing made multiple repeatable tests difficult to obtain. To obtain repeatable and economical trajectories of a test-unit to use for data analysis it was proposed that experiments, similar to what was performed on the sled track, be performed on a large centrifuge. On a centrifuge, test-units undergo a known trajectory continuously with a known angular velocity. Each revolution may represent an independent test which may be repeated many times over for magnitudes of data practical for statistical analysis. For this phase of the study, a series of experiments were conducted^b at Sandia National Laboratories' large outdoor centrifuge facility. A 3.6 meter long rocket shaped test-unit was affixed on top of a pedestal placed at the end of the 10.7 meter centrifuge arm (Fig. 2).



Fig. 2. Speckled test-unit affixed to 10.7 meter arm on the outdoor centrifuge at Sandia National Laboratories

Test-unit mounting hardware was designed to withstand a static acceleration of up to 10g. With a test radius of 10.532 m from the center of rotation to the centroid of the test-unit an angular velocity of 3.052 rad/s (0.4886 rev/s, 29.160 RPM) was used for testing; the corresponding tangential velocity to this angular velocity is 32.144 m/s. The actual angular velocity and acceleration obtained for the duration of centrifuge operation is shown in Fig. 3. The centrifuge was brought to test speed in 130 seconds and set to idle for 500 seconds before data collection began. This ensured that centrifuge speed was at its most stable velocity and that laser trackers were locked on to the target. After the 630 seconds, laser trackers began recording position and image data while a count was started for a trigger to synchronize high-speed digital cameras and digitizing systems. Laser tracker data was captured for 16 seconds, digitizer data was recorded for 10 seconds, and camera data was recorded for 7 seconds. It should be noted that DLTDIC data analysis was performed for a 0.295 second subset of these times. During the 16 second window, the average angular velocity of the test-unit was determined to be 29.065 RPM with a standard deviation of 0.545 RPM. These values were obtained from the analysis of speed data measured by two separate sources independent of the system under study.

^b February and March, 2008

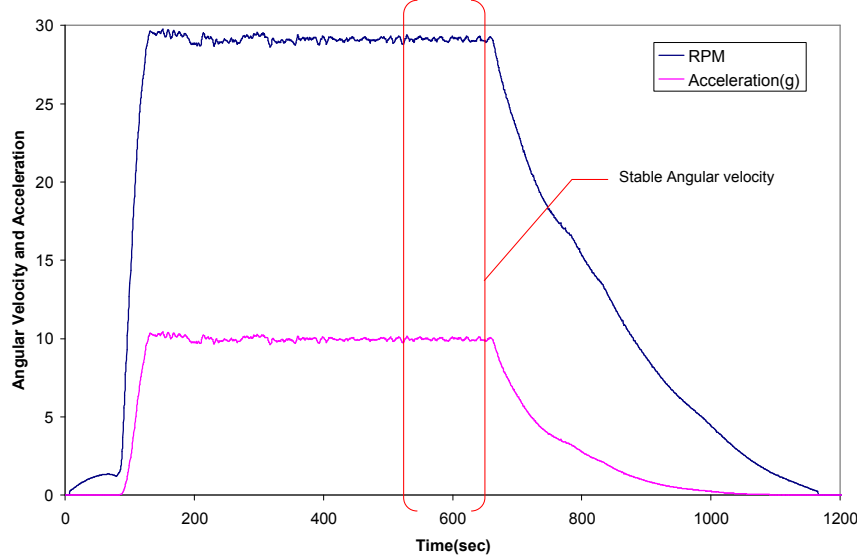


Fig. 3. Time history of angular velocity and centrifugal acceleration for the duration of centrifuge operation

Four independent measurement sources were used to determine “Ground Truth” test-unit trajectory independent from the laser tracking systems. The primary measurement system was a stationary DIC system capable of measuring the full-field position of the side of the test-unit within a 13.7 meter field-of-view (FOV). This FOV equates to approximately 60 degrees of test-unit travel. The second measurement source included two incremental encoders directly attached to the centrifuge shaft, a 5000 pulse per revolution incremental encoder, and a 900 pulse per revolution incremental encoder. The raw square wave output from the 5000 pulse per revolution encoder was directly recorded on a digitizing system operating at sample rate of 100 kHz, more than adequate to capture 2443 Hz square wave signal generate by the 5000 pulse per revolution encoder running at 0.4886 rev/s. To obtain a measurement of angular velocity, the frequency output of the 900 pulse per revolution encoder was measured using a calibrated frequency counter. When applying this technique, frequency varies linearly with rotational velocity; and the frequency may be easily scaled and recorded as a measure of rotational velocity. The third measurement source consisted of a single Phantom^c V7 digital camera mounted in an instrumentation rack located at the center of rotation with a moving FOV that included the test-unit and quadrille markers accurately located on the centrifuge test arena wall. The markers on the centrifuge arm, test-unit and centrifuge arena wall were measured using a laser based coordinate mapping machine (CMM). The fourth measurement source included two tri-axial accelerometers mounted on the test-unit. One accelerometer was mounted directly above the center of the test-unit while the other was mounted on the aft end of the test-unit. Accelerometer signals were recorded on the same digitizing system as the raw square wave signal from the 5000 pulse per revolution encoder.

The test-unit was painted with a speckle pattern containing quadrille markers embedded within the pattern. The markers are used to register the full-field DIC results with the test-unit and with a rigid-body description of the centrifuge arm. Tests were conducted at three different ranges: 222.5 m, 518.2 m and 1.000 kilometers. The lenses for the three different ranges were 800 mm, 2000 mm and 4000 mm, respectively. The trackers were positioned such that the angle between them was approximately 40 degrees at the three different ranges. The laser tracker lenses, stationary DIC system camera locations with 85mm lenses, and laser tracker positions were all chosen so that speckle pattern dot size^d would be ideal for both the stationary and the laser tracker cameras. This was simplified by using high resolution Phantom V10^e cameras for the stationary DIC system and Phantom V7^f cameras for laser trackers. This camera and lens arrangement allowed for the horizontal FOV of the stationary and laser trackers cameras to be approximately 13.7m and 4.6m respectively (Fig. 4).

^c Vision Research, Wayne, New Jersey, www.visionresearch.com

^d The nominal dot size of the speckle pattern is 3 to 5 pixels per speckle dot

^e Resolution = 2400x1600

^f Resolution = 800x600

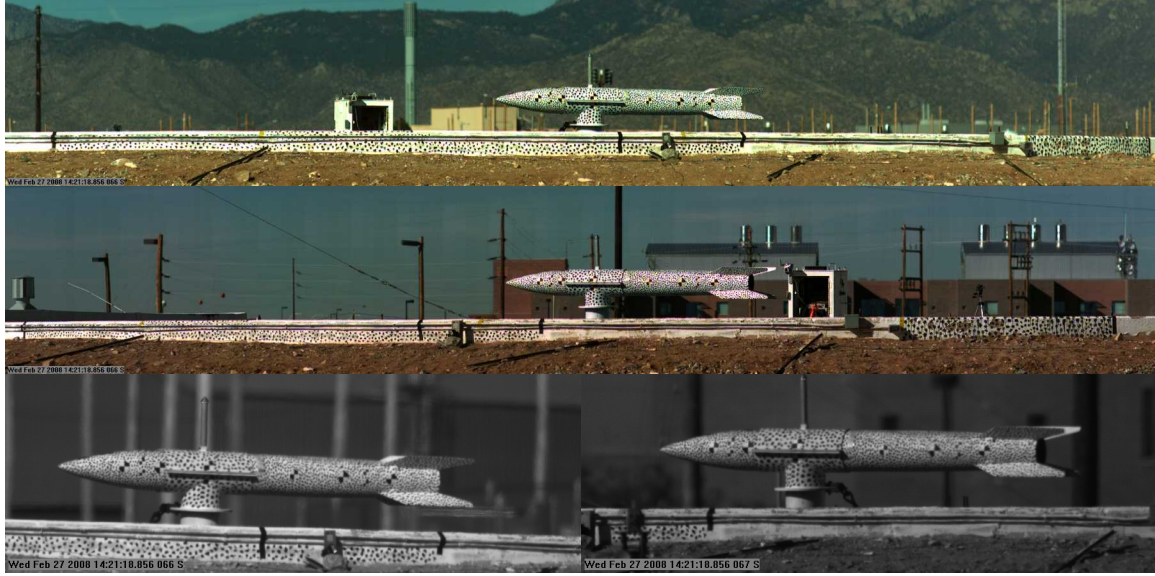


Fig. 4. Images from stationary DIC system (top and middle) and image from left and right laser tracker (bottom 2).

The test-area is defined as the arc spanning E-30 degrees to W-30 degrees. Each test contains at least one pass, if not more. Fig. 5 shows an overhead view of the test layout. The world coordinate system was defined to be nearly identical with the coordinate system used by the laser trackers. The origin is located at the center of rotation of the centrifuge arm. It was established by fitting a circle to position data collect from the end centrifuge the arm using the CMM. The center of the circle and its normal defined the direct of the Z-axis. The origin was translated along Z-axis to coincide with the top of the instrumentation rack located at the center of rotation. The positive Y-axis was select to bisect the locations of each tracker on the first test and to be perpendicular to the Z-axis. The X-axis is orthogonal to the Y-Z plane following the right hand rule. This results in a world coordinate system where the X-axis points generally to west, the Y-axis points generally south and the Z-axis points up.

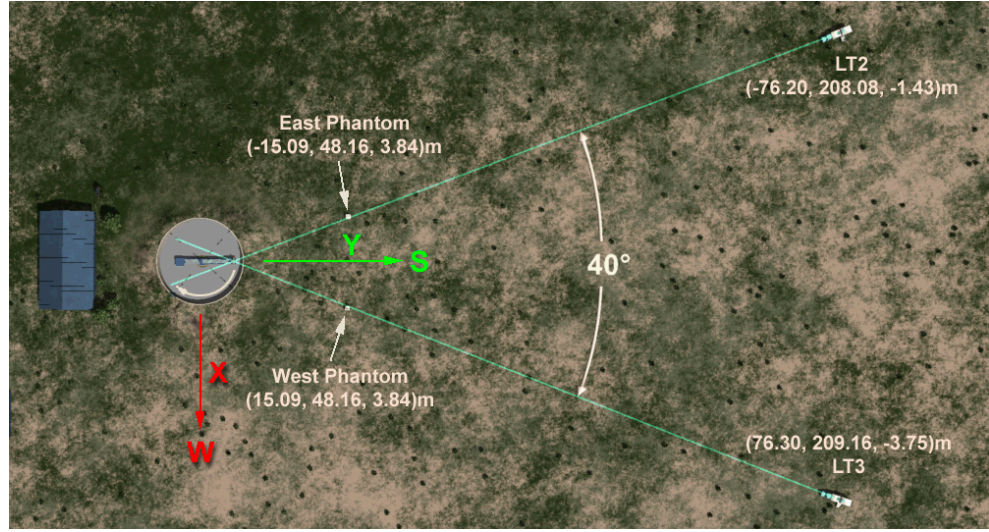


Fig. 5. Over head view of experimental setup for first position (220.5 m) of tests.

4. TEST DATA

For each day of testing, atmospheric data composed of temperature, wind speed and direction, pressure, humidity, and turbulence strength (C_n^2) were collected. Before each day of testing, the stationary DIC system as well as the laser tracker DIC systems were calibrated using a 2.4 square meter calibration grid. At the end of each day of testing, the

centrifuge arm was placed at 7 static positions that spanned ± 30 degrees off of the center line between the trackers and the stationary DIC system. At each of the static arm positions, the laser trackers were locked on to the retro reflector located on top of the test-unit (Fig. 4) and TSPI data was collected. In addition, 21 images were collected from the laser tracker cameras, the stationary DIC cameras, and the camera located at the center of the arm. Finally, the position of the arm was captured by measuring 8 quadrille markers located along the length of the arm^g.

During the day, we conducted several tests on the centrifuge. Image data were collected from each laser tracker, the stationary DIC system, and the camera at the center of the arm along TSPI data collected by the trackers. Data were synchronized between laser trackers, digital cameras, encoders and accelerometers using satellite IRIG^h timing, a shared trigger signal, and shared reference points on the centrifuge arena wall. A one pulse per revolution encoder signal was used to trigger ground-based DIC cameras, on-board camera and the digitizing system. The digitizing system recorded the trigger signal itself, the raw 5000 PPR encoder signal, accelerometer data, and the raw IRIG carrier signal. Each camera and both laser tracking systems record IRIG time with each sample of data.

4.1 Coordinate frame alignments

A CMM was used to collect static measurements of centrifuge and test-unit geometries. This included the measurement of 168 points on the wall of the centrifuge, static positions of the arm, inboard and outboard quadrille markers on the test-unit, and pass-points used for aligning each day's measurements with the world coordinate frame. The data from the CMM was analyzed using a 3D application called Spatial Analyzerⁱ. Some of its basic capabilities include point set alignment, construction of coordinate frames, lines, circles, etc., and report generation. The data from the CMM and Spatial Analyzer were used extensively to align and analyze data collected from the stationary DIC and DLTDIC systems as well as the centrifuge and test-unit geometries. An image of the spatial data for the centrifuge and static arm positions are shown in Fig. 6

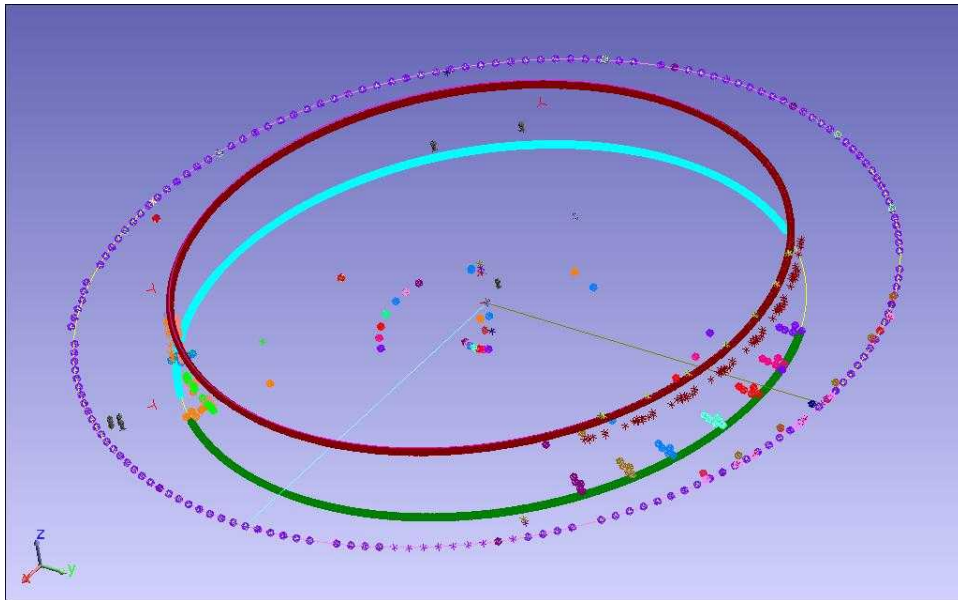


Fig. 6. Image captured from Spatial Analyzer showing coordinate mapping machine (CMM) and Laser Tracker data.

The full-filed data provided by the stationary DIC system and the DLTDIC system are relative to independent coordinate frames established by each system. The coordinate frame established by the stationary DIC system is located at the center of the baseline between the cameras. The X-Z plane is coplanar with the three point plane formed from the origins of each camera and the estimated intersection of rays projected from the origin of each camera through their optical centers. The Y-axis is normal to the X-Z plane and follows the right-hand rule. The coordinate frame established by the DLTDIC system coincides with the coordinate frame established by each laser tracker during their calibration process.

^g The quadrille markers were placed along the arm in such was to as to keep them from being co-linear with the arm.

^h Inter-Range Instrumentation Group see <http://en.wikipedia.org/wiki/IRIG> and <http://www.irig.org/>

ⁱ Spatial Analyzer is a software product of New River Kinematics <http://www.kinematics.com/products/sa/index.html>

In order to align the full-field results from each system with the world coordinate frame, we processed the full-field data collected from the stationary DIC and DLTDIC systems at the end of the testing day. The 3D point locations corresponding to the outboard quadrille markers on the test-unit were then extracted for each of the static locations. These locations were aligned with a set of constructed points corresponding to the markers on the test-unit at the static locations. In other words, since we did not measure the test-unit markers at each of static arm locations, we construct a set of outboard test-unit points relative to the arm at each of the static positions. The transformations required to align the static test-unit points from each system were then applied to the full-field data of each system.

4.2 Accelerometer Data

The accelerometer mounted on the aft end of the test-unit was found to measure greater levels of vibration than the accelerometer mounted on the forward end of the test-unit (Fig. 7); this was anticipated due to the free hanging configuration of the aft end of the test-unit. The aft mounted accelerometer measured 0.111grms in the radial axis, 0.137grms in the Z-axis and 0.034grms in the tangential direction. The forward mounted accelerometer measured 0.062grms in the radial axis, 0.031grms in the Z-axis and 0.024grms in the tangential direction. Frequency analysis was performed on the vibration data to determine the source of vibration, potential resonant frequencies and the expected magnitudes of displacement at these key frequencies. Vibration was determined to be independent of the 0.4886 Hz rotational frequency of the centrifuge. The frequencies that were found to have higher than average energy content were determined to be at 10, 15, 35, and 50 Hz (Fig. 7). These frequencies were more likely to be excited by the structural dynamics of the test-unit and mounting hardware rather than the centrifuge. The 10Hz vibration on the aft mounted accelerometer in the tangential direction encountered the greatest vibration induced displacement of 60.98 μ m, the 15Hz vibration on the forward and aft mounted accelerometers in the radial direction encountered the next highest vibration induced displacement of 50.44 μ m. These displacements are very small relative to the resolution of the DLTDIC technique and will be enveloped within the noise of the DLTDIC analysis results.

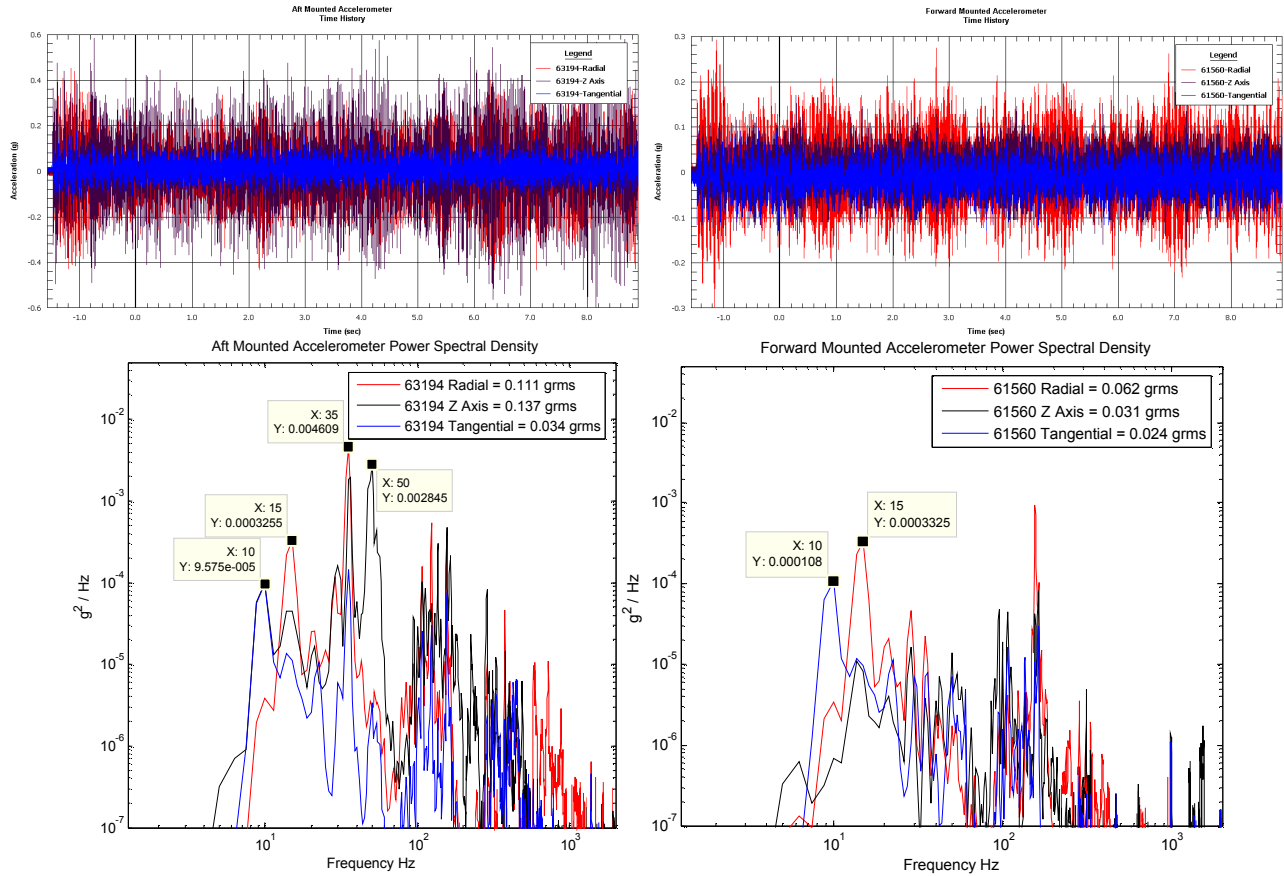


Fig. 7. Time history and frequency analysis results of aft (left) and forward (right) mounted tri-axial accelerometers

4.3 Centrifuge Based Time Space Position Information

The data from centrifuge based TSPI measurements obtained from the on-board phantom camera and shaft mounted encoder clearly show the repeatability of test-unit position over seven cycles (Fig. 8). The position of the test-unit's centroid at t-zero (IRIG 21:16.678980) is denoted by blue crosshairs. At t-zero a signal was transmitted that synchronously triggered all measurement systems with the exception of laser trackers which were triggered manually. The data from the trackers were synchronized using IRIG time. Fig. 8 also depicts the range of data that was used for DLTDIC analysis, this section of data is denoted by the 0.295 second window shown between the green \times (IRIG 21:18.706066) and the red \circ (IRIG 21:19.001066).

Position data in the X- and Y- axes matched well between both sources, agreeing with what was expected. The ensemble was split into seven sections, each section containing one complete cycle of data. An average TSPI was calculated from these seven sections followed by each sections deviation from the average. The standard deviation between each of these sections was determined to be 0.0742 m for the X data and 0.0707 m for the Y data.

The position and uncertainty of the centroid in the Z-axis could not be as easily defined from the on-board measuring systems. The on-board phantom was the only source of centrifuge based position in the Z-axis, and there was not phantom data available beyond T-0.9683 seconds. To overcome these challenges and provide data for comparison against DLTDIC results the Z-axis data from the phantom was filtered at 50 Hz and extended an additional three cycles. This was assumed to be reasonable since X and Y data was shown to be consistent through seven cycles and the Z data that was available showed consistency amongst its three cycles. Z data indicates that the centroid of the test-unit dropped 0.0237 m below its static height and oscillated about that offset.

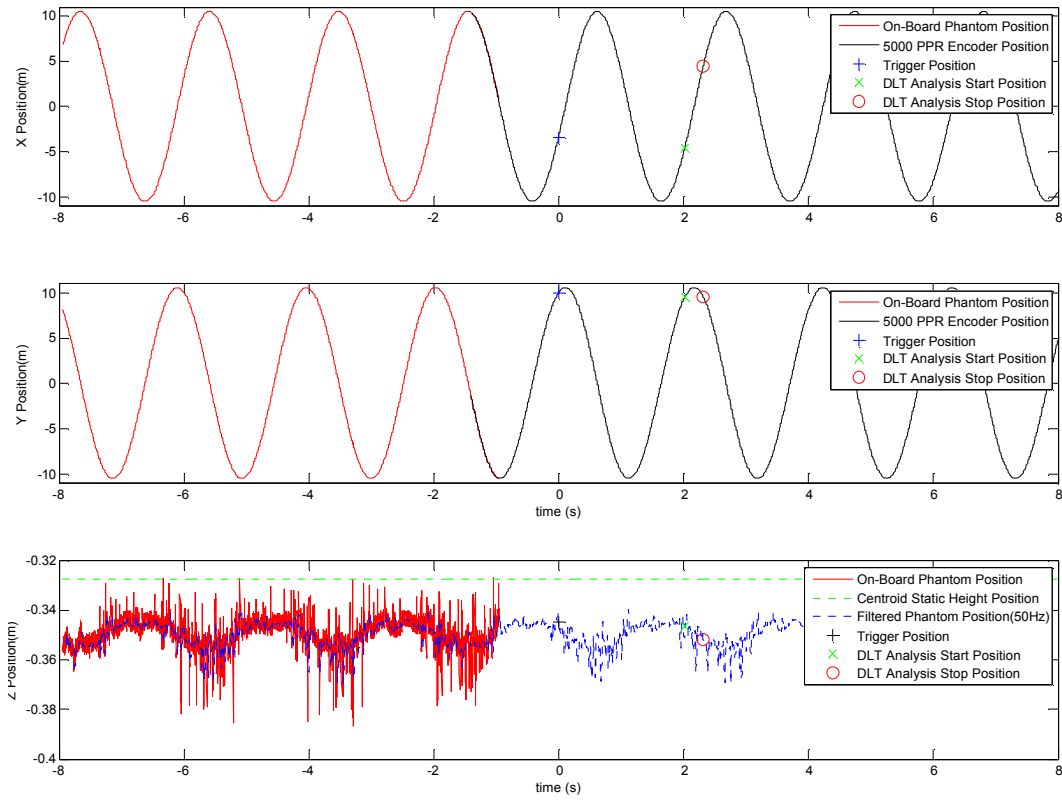


Fig. 8. Centrifuge based TSPI of test-unit centroid

The frequency analysis performed on X and Y data was optimized to provide high resolution frequency characterization. The results in Fig. 9A indicate a $0.4825 (\pm 0.045)$ Hz oscillation frequency for both the X- and Y- axis position data. This frequency agrees well with the 0.4886 Hz that was designed into the experiment. Time history for Z data appeared to have higher frequency content and was analyzed to characterize a broader frequency range. Frequency analysis of Z

data (Fig. 9B) gave no clear indication of any specific frequency peak but the frequency content of each cycle was shown to be consistent. These results did not match the rotational frequency of the centrifuge or any of the frequency content reported by the accelerometers that were measuring the same axis.

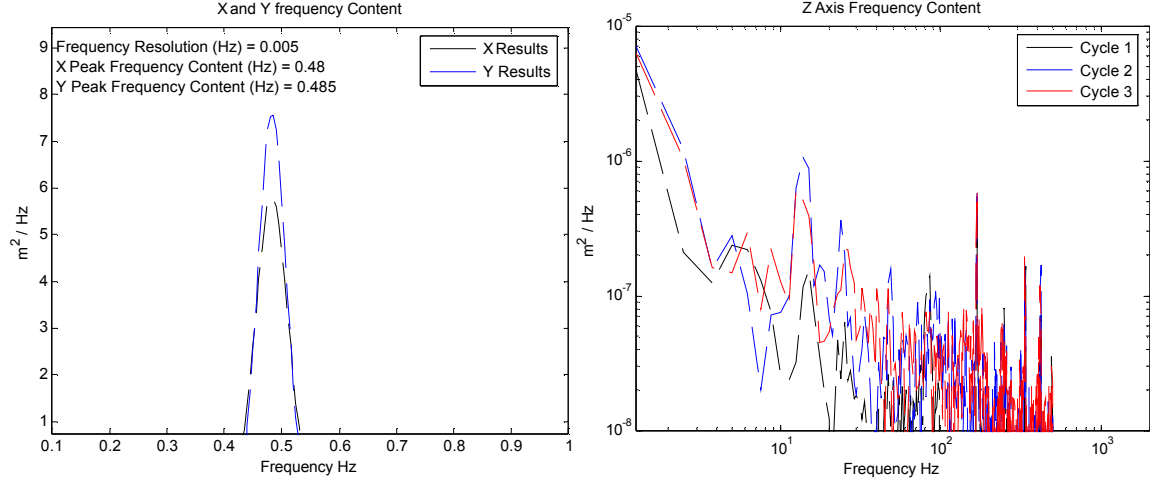


Fig. 9. (A) Frequency content of X and Y data

(B) Frequency content of Z data

5. RESULTS

The data presented here are the results from Test-Pass2. That is, they are from the second pass of the test-unit through the test area after the trigger. It should be noted that the results from both the stationary DIC and DLTDIC systems are unfiltered. As one would expect, the filtered results are somewhat better; but we wanted to present data without further processing. The TSPI for the centroid of the test-unit for both systems are plotted along with ground truth as evaluated from the centrifuge's encoder and on-board camera (see section 4.3) are shown in the top 3 subplots on the left half of Fig. 10. The orientation of the test unit relative to the world coordinate frame is plotted in the top 3 subplots on right half of Fig. 10. Unfortunately, we did not have an independent method for evaluating the true orientation of the test-unit. Consequently, we assumed that test-unit, centrifuge arm, and pedestal would behave as a rigid body and that the expected rotation about Z from X would be governed by the arm position. The expected rotations about X and Y were selected to remained fixed as evaluated from the CMM data. This may not be a valid assumption as the test-unit experiences static accelerations up to 10g during test.

The TSPI data shows close agreement with the expected results. The large spike in the Z position is due to a noise spike in Z position reported by laser tracker 3 (LT3). We could have corrected this error or before processing the DLTDIC data, but we decided to leave it in. The offset in Z and the changing slope reported by the DIC and DLTDIC systems may be caused by coordinate system alignment errors. We are still looking into the cause of these errors.

Difference errors between Ground Truth and the DIC and DLTDIC systems are shown in the bottom 6 subplots of Fig. 10, with TSPI errors shown on the left and the attitude errors shown on the right. The difference errors between the stationary DIC and the DLTDIC system are also shown in Fig. 10. The blue and green plot lines show the error of the DIC and DLTDIC systems relative to Ground Truth. The red plot line shows the error between the DIC and DLTDIC systems. The mean and standard deviation of the errors are shown in Table 1.

Will discuss error and error sources here

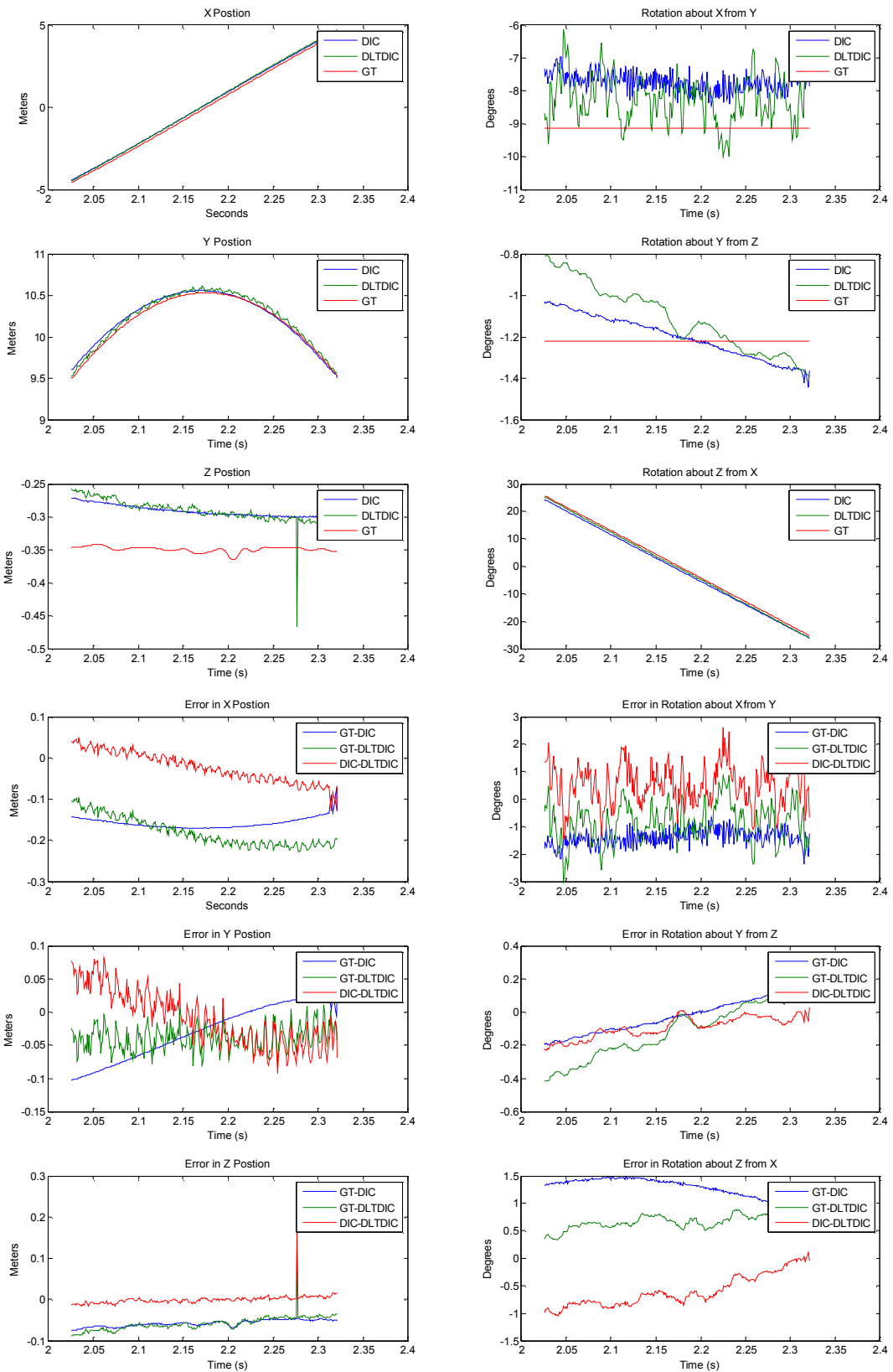


Fig. 10. Comparison (top 6) and error (bottom 6) plots of Stationary DIC system, DLTDIC and Ground Truth (GT) data

Error data for Test2-Pass2		Mean Error			Standard Deviation of Errors		
TSPI (in meters)		X	Y	Z	X	Y	Z
GT-DIC		-0.1577	-0.0293	-0.0579	0.0136	0.0408	0.0077
GT-DLTDIC		-0.1806	-0.0390	-0.0585	0.0346	0.0185	0.0169
DIC-DLTDIC		-0.0229	-0.0098	-0.0006	0.0368	0.0416	0.0117
Attitude (in degrees)		Rx from Y	Ry from Z	Rz from X	Rx from Y	Ry from Z	Rz from X
GT-DIC		-1.3969	-0.0232	1.2740	0.2970	0.1035	0.1893
GT-DLTDIC		-0.8606	-0.1150	0.6732	0.7060	0.1605	0.1296
DIC-DLTDIC		0.5363	-0.0919	-0.6009	0.7361	0.0630	0.2851

Table 1. Table showing the error data for Test2-Pass2 of the Centrifuge DLT DIC experiments

6. CONCLUSIONS AND NEXT STEPS

The initial results for this phase of the feasibility study are promising. We have been able to evaluate a preliminary accuracy estimate of the DLTDIC technique for the close in range at 220.5 m. We are in the process of analyzing the intermediate and long range experimental data. The image distortions in the long range (1 kilometer) images caused by the atmosphere may be too great for the DLTDIC technique and thus will require further processing to mitigate atmospheric distortions.

The error results are...

The spatial data aligned and analyzed with Spatial Analyzer are at the heart of the results reported later in this document. As such, measurement errors both systemic (bias) and random (precision) propagate through to the end results of the accuracy study. At this point, we believe the larger errors are the result alignment errors and inconsistent CMM operations. However, all is not lost. We feel that given the data we have collected, can do a better job on alignments.

Even though results presented in this document did not asses errors through strong turbulence, the results we obtained so far are promising. Further refinement of the technique, including a complete model for the camera and mirror system, as well as the use of image features as additional information to update the calibration in each frame, are expected to further improve the results and make the technique applicable to a wide variety of problems.

At this point we are pursuing the following next steps:

1. Continue to analyze the data from the current study and report results.
2. Investigate the value of dynamically updating the calibration using known target characteristics (i.e., the speckle pattern itself), fixed calibration boards, and/or known points in the field of view.
3. Experiment with using data produce by an enhanced DIC algorithm, which updates the reference image throughout the data acquisition to allow surface measurements of rotating test-units.
4. Add processing techniques to evaluate environmental dynamics (e.g., shockwave duration, spin rate, etc).
5. Incorporate atmospheric mitigation methods to reduce image distortions to enhance the possibility of measuring surface strain.
6. Add slave tracker to the 2 tracking systems to improve 6 degree of freedom sensitivity and operating range.
7. Replace laser ranger with a new pulsed picosecond Raman laser ranger system (Institute of Applied Physics, Nizhny Novgorod, Russia) to provide range accuracy on the order of cm. Add atmospheric mitigation technologies and hot spot tracking enhancements (University of Maryland Intelligent Optics Lab).
8. Perform sled ejector tests and missile tests.

ACKNOWLEDGEMENTS

The authors would like to thank the following people: Ed Bystrom for collecting the stationary DIC data, Dale Shamblin and Duane Patrick for operating the laser trackers during centrifuge tests and calibration data gathering, Al Sehmer for his 3D renditions and animations of the centrifuge test, and the centrifuge staff for operating the centrifuge.

Sandia is a multi-program laboratory operated by Sandia Corporation, a Lockheed Martin Company, for the United States Department of Energy under contract DE-AC04-94AL85000.

REFERENCES

1. T.L. Brown, D.L. Patrick, D.L. Shamblin, and T.J. Miller, "Next generation laser tracker concepts", *Target-in-the-Loop: Atmospheric Tracking, Imaging, and Compensation*, M.T. Valley and M.A. Vorontsov, Vol.5552, pp. 133-146, SPIE – The International Society for Optical Engineering, Bellingham, Washington, 2004.
2. H.W. Schreier, T.J. Miller, M.T. Valley, and T.L. Brown, "Application of stereo laser tracking methods for quantifying flight dynamics", *Atmospheric Optics: Models, Measurements, and Target-in-the-Loop Propagation*, S.M. Hammel, A.M.J. van Eijk, M.T. Valley and M.A. Vorontsov, Editors, Vol.6708, pp. 67080J, Proceedings of the SPIE – The International Society for Optical Engineering, Bellingham, Washington, 2007
3. G.S. Phipps, "Optical Analysis of a Gimbaled Mirror System", Sandia National Laboratories, Albuquerque, NM, SAND83-1123, July 1983.
4. G.S. Phipps, "A More Exact Analysis of Sandia Laser Tracker Data", Sandia National Laboratories, Albuquerque, NM, SAND94-0766, May 1994.